Original Research

The peripheral cannabinoid receptor 1 antagonist VD60 efficiently inhibits carbon tetrachloride-intoxicated hepatic fibrosis progression

Yan Wei[1], Xiao-li Kang[1] and Xu Wang[2]

[1]Department of Ophthalmology, Xinhua Hospital, Shanghai Jiao Tong University School of Medicine, Shanghai 200093, People's Republic of China; [2]Department of Oral and Maxillofacial-Head and Neck Oncology, College of Stomatology, Ninth People's Hospital, Shanghai Jiao Tong University School of Medicine, Shanghai 200011, People's Republic of China
Corresponding authors: Xu Wang. Email: wxwxw2004@126.com; Xiaoli Kang. Email: clove_lau@hotmail.com

Abstract

This study investigated a peripheral selective CB_1 antagonist 3,4,22-3-demethoxycarbonyl-3-hydroxylmethyl-4-deacetyl-vindoline 3,4-thionocarbonate (VD60) that efficiently inhibited hepatic fibrosis with lower psychological side effects. A competitive radiolabeled ligand binding experiment and 3′-5′-cyclic adenosine monophosphate (cAMP) response element-driven luciferase analysis were performed to evaluate the antagonistic activity of VD60. Cell viability and collagen production were examined in the human hepatic stellate cell (HSC) line LX-2 and primary cultured rat HSCs. The antifibrotic effects of VD60 were investigated in a CCl_4-induced liver fibrosis mouse model. The concentration of VD60 in the blood and the brain was determined by high-performance liquid chromatography–mass spectrum analysis. Furthermore, the potential underlying mechanisms of VD60 were investigated by Western blot. VD60 selectively competed with the radiolabeled CB_1 agonist to bind to CB_1. VD60 antagonized CB_1 agonist-induced Akt phosphorylation and increased the accumulation of intracellular cAMP. VD60 strongly reduced the expression of α_2(I) pro-collagen mRNA and exerted potent antiproliferative effects on primary HSCs and LX-2 cells. The inhibition of reactive oxygen species production and phosphorylation of Akt, extracellular-signal-regulated kinase (ERK), and Smad3 may explain the underlying mechanisms behind the antiproliferative effect of VD60. Moreover, the *in vivo* antifibrotic activity of VD60 was confirmed in a CCl_4-induced liver fibrosis mouse model. Most importantly, the concentration of VD60 in the peripheral blood was much higher than in the brain, suggesting that VD60 could act as a novel peripheral CB_1 antagonist to efficiently inhibit hepatic fibrosis and could be used as a lead compound with low brain side effects in peripheral antifibrotic agents.

Keywords: Cannabinoid receptor, hepatic fibrosis, peripheral antagonist, hepatic stellate cell

***Experimental Biology and Medicine* 2014; 239: 183–192. DOI: 10.1177/1535370213514922**

Introduction

Hepatic fibrosis is a severe public health problem worldwide.[1] Patients with hepatic fibrosis risk life-threatening complications, including portal hypertension, liver failure, and incident hepatocellular carcinoma.[2] The fibrogenic process is a common response to chronic liver injury that is characterized by the intense accumulation of activated hepatic stellate cells (HSCs). Although some antifibrogenic strategies have been developed to reduce fibrogenic cell accumulation by blocking their proliferation and/or inhibiting extracellular matrix synthesis or enhancing its degradation,[3] effective antifibrotic therapies are still lacking. Therefore, new targets for antifibrotic drug design are urgently needed.

Cannabinoid receptors belong to the G-protein coupled receptor superfamily, and their ligands are known as cannabinoids or endocannabinoids.[4] To date, two cannabinoid receptors, CB_1 and CB_2, have been identified. Although the CB_1 is mostly expressed in the central and peripheral nervous systems,[5,6] recent evidence has suggested that CB_1 is also extensively involved in liver diseases, such as Hepatitis C viral infection,[7] alcoholic liver disease,[8,9] and hepatic fibrogenesis.[10–14] These receptors were found to be upregulated in activated HSCs and human liver sections with various chronic diseases, while inhibiting CB_1 by gene knockout or pharmacological inhibition significantly attenuated fibrosis.[15,16] These findings suggest a novel role for a CB_1 antagonist for treating hepatic fibrosis, which has been gradually confirmed by the growing evidence that

selective CB_1 antagonist efficiently alleviates hepatic fibrosis and its complications.[4,17]

Rimonabant is the first reported CB_1 antagonist, which was first used clinically to ameliorate progressive obesity and prolonged associated metabolic indices.[18–20] Although rimonabant decreases appetite by inhibiting CB_1 signaling in the brain and increases energy consumption by repressing CB_1 in the peripheral tissue, the drug was suspended in 2008 due to its potential risk of psychiatric disorders. To date, many chemicals with similar pharmacophores to that of rimonabant have been synthesized as CB_1 antagonists. Most of them are inverse agonists that stimulate signal transduction in the absence of receptor stimulation and accumulate easily in the brain.[21] New types of peripheral antagonists with distinct novel structures from that of rimonabant have become valuable for the re-evaluation of the potential clinical use for CB_1 antagonists for treating hepatic fibrosis.[22]

In the current work, we discovered a novel compound, 3,4,22-3-demethoxycarbonyl-3-hydroxylmethyl-4-deacetylvindoline 3,4-thionocarbonate (VD60), as a peripherally specific CB_1 antagonist with distinct structure and potent antihepatic fibrotic activities by randomly screening against our in-house compound library (Figure 1(a)).

Methods and materials

Compounds

Unless otherwise mentioned, all chemicals and materials were received from commercial suppliers without further purification. CP55,940 was purchased from Sigma-Aldrich; AM630, arachidonyl-2-chloroethylamide (ACEA), and rimonabant were purchased from Tocris. [^{3}H]CP55,940 was purchased from PerkinElmer.

Chemical data

The following data describe the results of nuclear magnetic resonance of VD60: ^{1}H NMR ($CDCl_3$, 300 MHz) δ: 6.98 (d, J = 8.1 Hz, 1 H), 6.41 (dd, J = 8.1, 2.1 Hz, 1 H), 6.16 (d, J = 2.4 Hz, 1 H), 5.97 (dd, J = 9.6, 2.4 Hz, 1 H), 5.27 (d, J = 9.6 Hz, 1 H), 4.29 (s, 1 H), 4.00 (m, 2 H), 3.77 (s, 3 H), 3.57 (s, 1 H), 3.54 (m, 1 H), 3.29 (m, 1 H), 2.98 (s, 3 H), 2.72 (m, 2 H), 2.30 (m, 3 H), 1.69 (m, 1 H), 1.01 (m, 1 H), 0.23 (t, J = 7.5 Hz, 3 H).^{13}C NMR ($CDCl_3$, 75 MHz) δ: 192.1, 160.7, 153.9, 129.9 (2 C), 127.6, 123.6, 106.3, 97.9, 91.3, 85.3, 74.6, 70.9, 66.8, 55.6, 54.7, 53.2, 51.0, 44.0, 42.2, 42.0, 28.0, 7.8. High performance liquid chromatography (HPLC) purity: 100% (MeOH:H_2O 80:20; retention time: 8.46 min). HRESIMS (m/z) 429.1848 ($[M+H]^+$, $C_{23}H_{29}N_2O_4S^+$; cald. 429.1848).

Cell culture

HSCs were isolated from normal rat livers (male Sprague–Dawley rats, 400–450 g) according to the published approach.[23] All the experiments were performed using 6-day culture-activated HSCs. Human HSC line LX-2 was kindly provided by Professor Frideman (Mount Sinai School of Medicine, New York). The human hepatocyte LO2 cell line was obtained from the American Type Culture Collection. CHO cells over-expressing hCB_1 (CHO–hCB_1) or hCB_2 (CHO–hCB_2) were constructed according to the previous method.[24] Cells were maintained in Dulbecco's Modified Eagle Medium (DMEM) medium supplemented with 10% fetal bovine serum (Gibco), penicillin–streptomycin (50 U/mL, Gibco), and geneticin (0.5 mg/mL, Merck). The cells were cultured at 37°C in a humidified atmosphere with 5% CO_2 in air.

Cell membrane preparation

CHO–hCB_1 or CHO–hCB_2 was used for binding assay. To prepare cell membranes, cells were harvested by scraping, washed in phosphate-buffered saline (PBS) containing 1 mM ethylenediaminetetraacetic acid (EDTA) and Buffer A (320 mM sucrose, 10 mM 4-(2-hydroxyethyl)-1-piperazineethanesulfonic acid [HEPES], 1 mM EDTA at pH 7.4), and then Dounce homogenized. Cell homogenates were centrifuged at 1600 g for 10 min, and the supernatant was abandoned. The pellet was resuspended in Buffer A, homogenized and centrifuged as before, and then the supernatant was gathered by further centrifugation at 50,000 g for 2 h. The supernatant was discarded and the pellet was resuspended in Buffer B (50 mM HEPES, 0.5 mM EDTA, 10 mM $MgCl_2$ at pH 7.4), aliquoted and stored at –80°C.

Radioligand binding assay

The radiolabeled ligand binding assay was used for investigating the specific affinity of VD60 against CB_1 according to the published approach.[25] The assay was performed by incubating 10 mg/well CHO–hCB_1 cell membranes with either 1.7 nM [^{3}H]CP55,940 (PerkinElmer) alone or 1.7 nM [^{3}H]CP55,940 containing different concentrations of VD60 in 50 mM Tris, 2.5 mM EDTA, 5 mM $MgCl_2$, and 1 mg/mL bovine serum albumin buffer (pH 7.4) at 30°C for 90 min in a final volume of 200 μL. A concentration range of the tested compound (the known CB_1 antagonist rimonabant as a positive control or VD60) was added before the addition of [^{3}H]CP55,940. Unlabeled CP55,940 (10 nM) was used to define the non-specific binding for [^{3}H]CP55,940. After incubation, reactions were filtered onto GF/B filter mats presoaked in 0.05% polyethyleneimine. Filters were washed six times with ice-cold buffer (50 mM Tris, 2.5 mM EDTA, 5 mM $MgCl_2$, pH 7.4), then air-dried and the radioactivity was counted in a Microbeta liquid scintillation counter (PerkinElmer).

cAMP response element (CRE)-dependent luciferase reporter gene assay

For the cAMP response element (CRE) driven reporter gene experiments, plasmid pTAL-CRE-luc that encodes firefly luciferase was co-transfected with pRL-SV40 vector (Promega) encoding renilla luciferase as an internal control by using Lipofectamine 2000 (Invitrogen) into CHO–hCB_1 cells.[26] After 6-h transfection, cells were incubated with 5 μM forskolin and the tested compounds for 18 h, and luciferase activities were determined by Dual Luciferase Assay kit (Promega) according to the manufacturer's instruction.

Western blot analysis

Western blot assay was carried out according to the standard approach.[27] After cells were lysed, proteins were

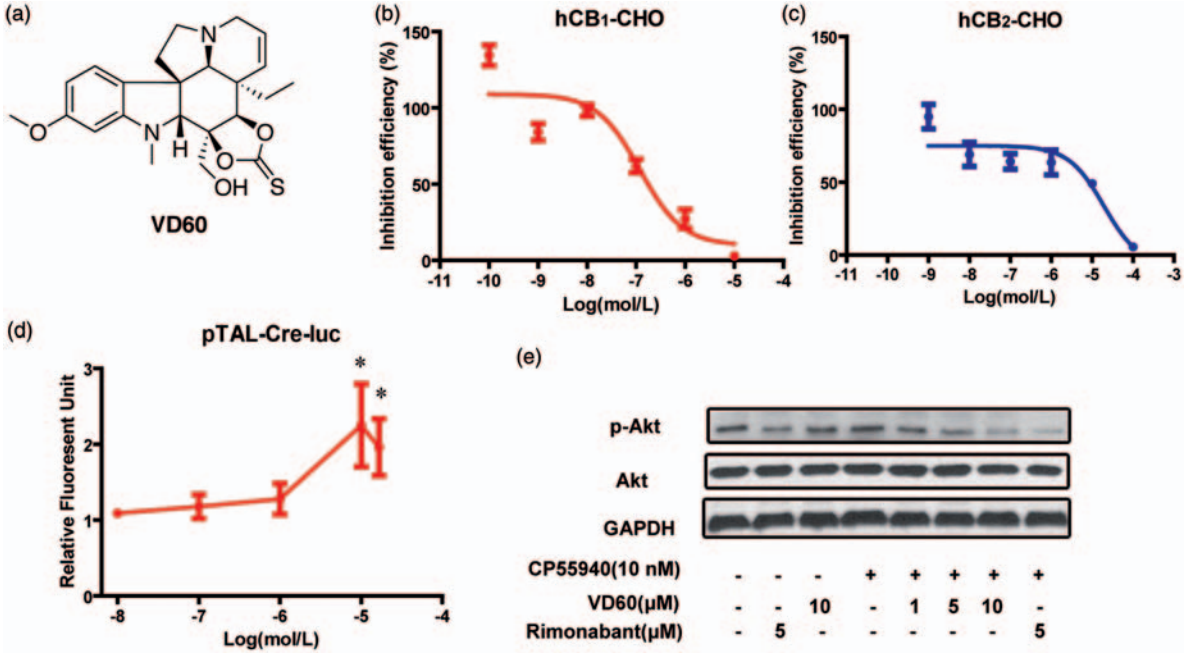

Figure 1 VD60 functions as an antagonist/inverse agonist of CB_1. **(a)** Chemical structure of VD60 (3,4,22-3-demethoxycarbonyl-3-hydroxylmethyl-4-deacetyl-vindoline 3,4-thionocarbonate). (b) VD60 competed with ^{3}H-labeled CB_1 agonist CP55,940 to bind CB_1 receptors isolated from CHO–hCB_1 cells. (c) VD60 was less competitive when competing with [^{3}H]-CP55,940 to bind CB_2 receptors isolated from CB_2-CHO cells. (d) In the luciferase assay, the CRE-driven luciferase signals in CHO–hCB_1 cells were increased by VD60 treatment (10 and 20 μM) for 18 h. Data were expressed as the mean ± SEM of three independent experiments. **(e)** CHO–hCB_1 cells were treated with the indicated concentrations of VD60 with or without 10 nM CP55,940 for 4 h. Compared with the dimethyl sulfoxide-treated control, CP55,940 increased the Akt phosphorylation. Co-incubation of VD60 with CP55,940 inhibited the CP55,940-activated Akt phosphorylation in a dose-dependent manner, similar to the activity of the CB_1 antagonist rimonabant (5 μM). *$P < 0.05$ compared to the control group. (A color version of this figure is available in the online journal.)

denaturized, separated on 10% Sodium dodecyl sulfate (SDS)-polyacrylamide gel, and electroblotted onto Hybond-C extra membrane (Amersham Pharmacia Biotech). The membrane was then stained with Ponceau S (Sigma-Aldrich) to verify the equal amount of sample loading, followed by incubation for 1 h at room temperature with 5% non-fat dry milk in T-PBS. The membrane was probed overnight at 4°C with primary antibody and then mixed with the horseradish peroxidise-conjugated secondary antibody diluted to 1:3000 (Dako Corporation). The bound antibodies were detected by enhanced chemiluminescence (ECL) using ECL kit (Amersham Pharmacia Biotech). The following primary antibodies were used: α-smooth muscle actin (SMA) (monoclonal antibody, dilution 1:200) (BOSTER), Akt and p-Akt (polyclonal antibody, dilution 1:3000) (Cell Signaling Technology), extracellular signal-regulated kinase (ERK)1/2 and p-ERK1/2 (monoclonal antibody, dilution 1:3000) (Cell Signaling Technology), Smad3 and p-Smad3 (monoclonal antibody, dilution 1:3000) (Cell Signaling Technology), glyceraldehyde 3-phosphate dehydrogenase (GAPDH) (polyclonal antibody, dilution 1:5000) (Sigma-Aldrich), CB_1 (polyclonal antibody, dilution 1:1000) (Abcam), CB_2 (polyclonal antibody, dilution 1:1000) (Abcam).

Cell viability assay

The sulphorhodamine B (SRB) assay[28] was performed to determine the antiproliferative effects of VD60 on rat primary HSCs and human LX-2 cells. In the assay, cells were seeded into a 96-well plate by 3000 cells per well and incubated overnight. The cells were treated with varied concentrations of tested compound in the presence of platelet-derived growth factor-BB (PDGF-BB) (20 ng/mL) for 72 h, fixed with 10% trichloroacetic acid, stained with 4 mg/mL SRB solution, and finally dissolved with 10 mM unbuffered Tris base. Cell viability was measured by detecting absorbance at 550 nm (BioRAD spectrophotometer). Each experiment was repeated for at least three times.

RNA interference

siRNA sequences against human cannabinoid CB_1 receptor and negative control siRNA were purchased from Genechemat. Transfection of siRNAs into LX-2 cells was performed 24 h after plating as previous report.[29] In brief, LX-2 cells were seeded at a density of 1×10^7 cells/100-mm Petri dishes the day before transfection to achieve 50–60% confluence. Transfections were carried out with 50 nmol siRNA duplex using Lipofectamine 2000 (Invitrogen) according to the manufacturer's instructions. After 6-h incubation, the transfection medium was replaced with serum-free medium. After 48 h, transfected cells were treated with compounds or medium for 24 h followed by lysis, harvest of proteins, and Western blot analysis.

Reactive oxygen species (ROS) production measurement

The intracellular reactive oxygen species (ROS) were detected using 2′-7′-dichlorofluorescein diacetate

(DCFH-DA) as a probe according to the reported method.[30] LX-2 cells were seeded into 96-well plates with cell density of 3×10^3 cells/well in complete DMEM media and cultured for 24 h. The cells were incubated with 5 μM DCFH-DA for 20 min at 37°C, washed twice with PBS, and preincubated with the known selective CB_1 agonist ACEA (0 or 5 μM, Tocris) at 37°C for 1 h followed by incubation with varied concentrations of tested compound for 2 h (37°C). Finally, 20 ng/mL PDGF-BB was added to induce ROS. The fluorescent intensity was then detected with GENios microplate reader (Tecan) using excitation and emission wavelengths of 485 and 535 nm.

RNA isolation, reverse transcription, and real-time polymerase chain reaction (PCR)

Quantitative PCR was carried out for measurement of mRNA levels. In the assay, total RNA was isolated by RNeasy Total RNA System (Qiagen) following the manufacturer's instructions. RNA (1 μg) was reversely transcribed to cDNA using ReverTra Ace reverse transcription kit (Takara). Real-time PCR was performed according to the standard protocol by SYBR Green real-time PCR Master Mix (Toyobo) and DNA Engine Opticon TM2 System (MJ Research). The following primer pairs were used: human α_2(I) procollagen, 5′-ACT CAG CCA CCC AGA GTG GA-3′ (sense) and 5′-TCT TGC AGT GGT AGG TGA TG-3′ (antisense)[31]; rat α_2(I) procollagen, 5′-AGA ATT CCG TGT GGA GGT TG-3′ (sense) and 5′-GAG GGA GGG GAC TTA TCT GG-3′ (antisense); human β-actin: 5′-GAT GAG ATT GGC ATG GCT TT-3′ (sense) and 5′-GAG AAG TGG GGT GGC TT-3′ (antisense); rat 18 s RNA, 5′-GTA ACC CGT TGA ACC CCA TT-3′ (sense) and 5′-CCA TCC AAT CGG TAG TAG CG-3′ (antisense)[15]; mouse transforming growth factor (TGF)β 5′-CCA CCT GCA AGA CCA TCG AC-3′ (sense) and 5′-CTG GCG AGC CTT AGT TTG GAC-3′ (antisense); mouse fibronectin 5′-ATG TGG ACC CCT CCT GAT AGT-3′ (sense) and 5′-GCC CAG TGA TTT CAG CAA AGG-3′ (antisense).

Chronic liver injury

In the chronic liver injury animal model, 40 C57/BL6 male mice at 8-week age were obtained from Shanghai SLAC Laboratory Animal Co. Ltd and maintained in a temperature controlled room at 25°C with a 12 h light–dark lighting cycle. Animals were allowed a standard pellet chow and water *ad libitum*. All the animals received humane care, and the experiments were performed according to the institutional ethical guidelines on animal care.

The antihepatic fibrosis assay for VD60 was carried out based on the CCl_4-intoxicated mouse model. The CCl_4-induced liver fibrosis was generated in 32 mice (8 mice each group) as described.[15] VD60 (10, 15, and 25 mg/kg, daily) was dissolved in Tween-80 (a final concentration of 3%) and intraperitoneally injected into mice daily. At the same time, the normal control group (eight mice) was treated with olive oil twice weekly and was intraperitoneally injected with vehicle (Tween-80) daily. After 4 weeks, animals were starved overnight and sacrificed 48 h after the last CCl_4 injection. Anesthesia was performed by intraperitoneal injection of chloral hydrate at a dose of 350 mg/kg.

Liver histology assay

Liver histology assay was performed according to the reported approach.[27] The liver specimens of mice were fixed in 10% formalin and embedded in paraffin. The tissue sections (4 μm) were stained with hematoxylin–eosin for routine examination or with Sirius red for visualizing hepatic collagen deposition.

In immunehistochemical analysis, the sections were deparaffinized and treated in citrate buffer for 10 min, followed by 0.3% hydrogen peroxide for 10 min and incubated with 5% bovine serum albumin for 30 min. The sections were incubated with anti-α-SMA primary antibody (1:200 dilution, BOSTER) overnight at 4°C. After the primary antibody had been rinsed, the sections were treated with the secondary biotinylated goat anti-rabbit antibody for 1 h at room temperature, and then incubated with ExtrAvidin-Peroxidase and rinsed with PBS. The specific binding indicated by diaminobenzidine was visualized with light microscopy.

Blinded to the study conditions, we quantified fibrosis from Sirius red-stained and immunohistochemical liver tissue sections by morphometric analysis with Image-Pro Plus software (MediaCybernetics, MicroMecanique). Values were the mean of five fields taken from liver section per mouse.

Hydroxyproline content detection

Liver collagen concentration was determined by measuring the hydroxyproline content in liver samples based on the previous method.[32] Briefly, liver samples were homogenized and hydrolyzed in 6 M HCl at 99°C for 15 min. After the sample temperature was decreased to room temperature, chloramine T was added to a final concentration of 2.5 mM. The mixture was then treated with 410 mM paradimethyl-amino-benzaldehyde and incubated at 60°C for 30 min. The concentration of hydroxyproline in each sample was determined spectrophotometrically at 560 nm using the standard curve generated from the known quantities of hydroxyproline. Each liver sample was measured in triplicate, and the mean value of hydroxyproline was used for analysis. The results were expressed as micrograms per milligram of wet tissue.

High performance liquid chromatography–mass spectra assay for VD60 levels in plasma and brain

After five C57/BL6 mice were injected intraperitoneally with 25 mg/kg VD60, blood was collected into heparin-pretreated Eppendorf tubes at different time points (0.25, 0.5, 1, 2, and 4 h). Blood samples and brain were immediately put on ice and centrifuged at 4°C (3000 rpm, 15 min). Plasma was stored at −80°C. Chromatographic column of SepaxHP-C18 (2.1 × 50 mm, 5 μm) was used for HPLC assay with CH_3OH–H_2O (2:98, 0.1% NH_4COOH), and CH_3OH–H_2O (90:10, 0.1% NH_4COOH) was used as the mobile phase. For mass spectrum (MS) detection, positive

electrospray ionization (ESI) mode, selected reaction monitoring (SRM) assay: m/z 429.1→188.0. The specificity of the assay was checked. The limit of quantification and limit of detection of the assay were 5 and 2 ng/mL, respectively. The tR (retention time) of VD60 was 5 min.

Data analysis

Each set of experiments was repeated at least three times. The results were expressed as mean ± SEM and analyzed either by Mann–Whitney test or analysis of variance. Data statistical analysis was performed with statistical analysis software SPSS 13.0. $P < 0.05$ was considered as the minimum level of significance.

Results

VD60 is a specific CB_1 antagonist/inverse agonist

A competitive radiolabeled-based assay was used to detect the antagonistic binding mode of VD60 to cannabinoid receptors. As shown in Figure 1(b), VD60 has been further confirmed to exhibit strong binding activity. The IC_{50} value against [^{3}H]CP55,940 binding CB_1 was 0.118 μM and the Ki value was 0.026 μM. The same values for CB_2 were 19.46 and 4.289 μM, respectively (Figure 1(c)).

As reported, most CB_1 antagonists are inverse agonists that increase intracellular cAMP accumulation, induce CRE binding protein phosphorylation through cAMP-dependent protein kinases, and mediate CRE-driven gene transcription.[33] We thus investigated the potential inverse agonistic behavior of VD60. The effects of VD60 on the intracellular cAMP level were detected by measuring CRE-dependent luciferase activity. As expected, treating cells with VD60 increased the CRE-dependent luciferase activity (Figure 1(d)), which is characteristic of a CB_1 inverse agonist.

In previous reports, CB_1 antagonism reduced Akt phosphorylation.[34] Therefore, we examined the potential effect of this compound on CP55,940-induced Akt phosphorylation in CHO–hCB_1 cells to further evaluate the antagonistic activity of VD60 against CB_1. As shown in Figure 1(e), VD60 decreased not only the 10 nM CP55,940-induced Akt phosphorylation in a dose-dependent manner, but also reduced the basal phosphorylation of Akt, similar to the action of the inverse agonist rimonabant. Taken together, the data suggest that VD60 functions as a receptor antagonist/inverse agonist.

VD60 inhibited HSC proliferation and ROS production

Due to the pivotal role of activated HSCs in hepatic fibrosis,[1] we evaluated the antiproliferative effects of VD60 on human LX-2 cells and rat primary HSCs. The results showed that VD60 inhibits the PDGF-BB-stimulated proliferation of both LX-2 cells (Figure 2(a)) and rat primary HSCs (Figure 2(b)) in a dose-dependent manner, while co-incubation with the specific CB_1 agonist ACEA[35] abolished the antiproliferative effects of VD60. VD60 was also tested on normal hepatocytes. Figure 2(c) shows that the antiproliferative effect of VD60 in the normal human hepatocyte cell line LO2 was much lower than that in LX-2, implying that VD60 efficiently treats fibrotic HSCs without causing cytotoxic effects in normal hepatocytes.

Incubating LX-2 cells with VD60 for 48 h decreased the level of α-SMA protein, which is a marker of HSC activation (Figure 2(d)). VD60 also inhibited two pathways, the canonical PI3 Kinase-Akt pathway and the ERK signaling pathway, that are linked to CB_1 antagonist-based anti-PDGF-BB effects. PDGF-BB stimulated ROS production and proliferation in HSCs, while VD60 dose dependently inhibited PDGF-BB-induced ROS (Figure 2(e)). The results show that ACEA counteracts the VD60-based reduction of ROS and confirmed its CB_1-antagonistic behavior.

To exclude other targets involved in VD60's antifibrotic effects, we examined the cell viability in CB_1 knockdown cells. As shown in Figure 2(f), CB_1 receptor was knockdown with specific siRNA transfection. However, 10 μM VD60 treatment for 48 h shows no further decrease in the cell viability assay (Figure 2(g)), suggesting there is no effect of VD60 via other targets.

We also performed comparison between VD60 and Rimonabant on their antifibrotic effects *in vitro*. Both compounds indicated no significant reduction on the CB_1 and CB_2 receptors in LX-2 cells (Figure 2(h)). However, they obviously decreased the cell viability (Figure 2(i)).

VD60 inhibited collagen production and extracellular matrix synthesis in HSCs

Subsequently, the effects of VD60 on the major components of extracellular matrix synthesis were also examined in HSCs. Quantitative RT-PCR analysis revealed that VD60 (10 μM) significantly inhibited TGFβ_1-induced transcription of the α_2 chain of type I procollagen mRNA in LX-2 cells (Figure 3(a)). Moreover, co-incubation with 5 μM ACEA reversed VD60-induced inhibition of α_2 (I) procollagen mRNA levels, suggesting that VD60 downregulated this gene by antagonizing the CB_1 receptor. We also examined the potential influences of VD60 on the relevant signaling pathways. As indicated, VD60 reduced the phosphorylation of Smad3 without altering its total protein levels (Figure 3(b)). Furthermore, both VD60 and Rimonabant reduced α_2 (I) procollagen mRNA levels (Figure 3(c)) in a similar way.

VD60 attenuated fibrosis progression in CCl_4-intoxicated mouse model

Intrigued by the ability of VD60 to inhibit collagen expression in HSCs, we further inspected the antifibrotic activity of VD60 *in vivo* in a CCl_4-induced hepatofibrotic mouse model. First, the compound's concentration in the plasma and brain was measured to examine the absorption and biodistribution of VD60 in the blood and the brain and to collect useful information for subsequent assays. As presented in Table 1, the concentration of VD60 in the brain was much less than that in the blood plasma at all time points, suggesting that VD60 has difficulty penetrating the blood–brain barrier and mainly accumulates in peripheral tissues. We next examined the ability of VD60 to inhibit fibrosis progression in a CCl_4-induced mouse model. The results showed that the vehicle group exhibited extensive formation of septa with some nodules, while the

VD60-treated group revealed limited formation of fibrotic septa (Figure 4(a)) and reduced α-SMA expression (Figure 4(b)). The quantitative data suggested that the fibrotic area was decreased by 40% in the VD60-treated group (25 mg/kg) compared with the vehicle group (Figure 4(c)); α-SMA expression in this group was also reduced (Figure 4(d)). Additionally, hepatic hydroxyproline (HYP) deposition in the VD60 (25 mg/kg)-treated group was decreased by 30% (Figure 4(e)). The results indicate that VD60 attenuated hepatic fibrosis in a CCl_4-induced mouse model of

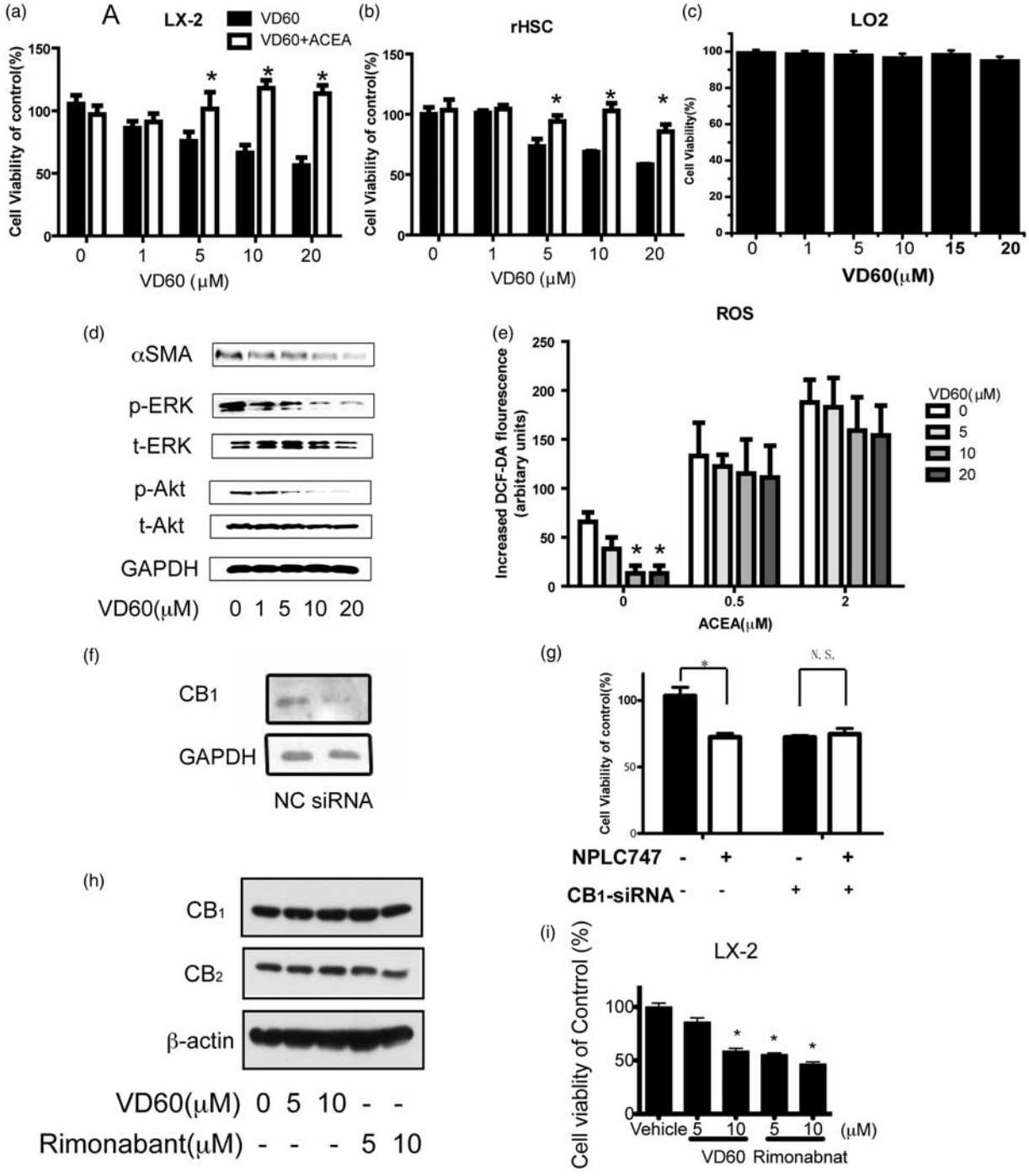

Figure 2 VD60 inhibits the proliferation of LX-2 cells and primary rat HSCs. (a) LX-2 cells and (b) rat primary HSCs were incubated with the indicated concentrations of the test compounds and 20 ng/mL PDGF-BB for 72 h. Cell proliferation was evaluated by the SRB method. VD60 inhibited proliferation of LX-2 cells and primary rat HSCs in a dose-dependent manner. ACEA (5 μM) reversed the VD60-induced reduction of proliferation. (c) VD60 had no influence on the proliferation of LO2 cells. Data are expressed as the mean ± SEM of four independent experiments. (d) After LX-2 cells were treated for 48 h with increasing concentrations of VD60 (1, 5, 10, and 20 μM), Western blot analysis was performed. VD60 significantly reduced α-SMA expression and the phosphorylation of ERK1/2, Akt, and Smad3. (e) In the LX-2 cells treated with PDGF-BB (20 ng/mL, 30 min), preincubation of VD60 (10 and 20 μM) decreased the levels of ROS compared to the vehicle group, while co-incubation with ACEA (5 μM) abolished the effect (*indicated $P < 0.05$ versus control). Data are expressed as the mean ± SEM of three independent experiments. (f) After the cannabinoid CB_1 receptor was silenced by CB_1-siRNA in LX-2 cells, VD60 could not indicate further inhibitory effect against cell viability (g). After indicated VD60 and Rimonabant incubation for 48 h, the CB receptors were not obviously influenced (h) and the cell viability was indicated (i) (*indicated $P < 0.05$ versus control).

hepatic fibrosis. Furthermore, we have examined the mRNA levels of two critical pro-fibrotic genes, TGFβ and fibronectin. VD60 treatment (25 mg/kg) significantly reduced both gene expression compared to the model group (Figure 4(f)).

Although the previous report states that single rimonabant injection can reduce food intake in both normal and obesity mice,[36] there was no significant difference in food intake between VD group and vehicle group (Figure 4(g)). These data are consistent with the effects of VD60 being mostly localized in the peripheral system.

Discussion

The endocannabinoid system is widely expressed in the human body and is involved in a variety of physiological functions. Since the identification of cannabinoid receptors, growing efforts have been put into determining their specific ligands. The discovery of CB_1 antagonists has greatly facilitated this research. CB_1 antagonists were first used clinically to treat progressive obesity. In addition to its anti-obesity effects, rimonabant was recently reported to improve metabolic syndrome and reduce the risk of fatty liver disease.[37,38] Moreover, CB_1 antagonists have also been used to control fatty liver induced by ethanol[39,40] or a high fat diet.[41] Therefore, discovering selective CB_1 antagonists with novel structures is important to create new treatments for these diseases. In this study, we found that VD60 acted as a potent CB_1 antagonist with a structure distinct from that of rimonabant and exhibited efficient antifibrotic activity.

Table 1 VD60 concentrations in the blood plasma and the brain

	Plasma	Liver	Brain	Brain/plasma ratio
15 min	707 ± 356	720 ± 327	153 ± 41	0.217
30 min	267 ± 142	274 ± 153	58 ± 25	0.219
1 h	257 ± 7.7	280 ± 37.8	53 ± 21	0.207
2 h	20 ± 7.7	19 ± 9.8	4.4 ± 1.1	0.22
4 h	4.9 ± 1.1	5.7 ± 2.6	BLQ	N/A
8 h	BLQ	BLQ	BLQ	N/A

BLQ: below the limit of quantification; N/A: no results.

VD60 is a selective antagonist that specifically antagonizes CB_1 over CB_2 when put up against the known CB_1 agonist CP55,940. Consistent with most of the reported CB_1 antagonists, VD60 also inhibited CP55,940-activated Akt phosphorylation. Additionally, VD60 increased cellular cAMP accumulation, which characterizes inverse CB_1 agonist activity.

Both *in vitro* and *in vivo* hepatic fibrosis models were used to evaluate the antifibrotic effects of VD60. The inhibition of HSC proliferation and collagen synthesis by VD60 has revealed its effectiveness against fibrosis because HSCs are considered to be the key component of fibrosis. Such antiproliferative effects were mediated by VD60's inhibition of PDGF-BB-induced ROS production and of key pathway activation (Akt and ERK1/2 phosphorylation). Moreover, VD60 reduced the $TGF\beta_1$-induced α_2 (I) procollagen mRNA expression, possibly due to its inhibition of Smad3 phosphorylation. Additionally, both the antiproliferative and anticollagen synthesis of VD60 could be reversed by treating with the selective CB_1 agonist ACEA, confirming that VD60 is a specific antagonist for CB_1. VD60 also attenuated fibrosis progression *in vivo*, as indicated by noticeable decrease in the fibrotic area and hydroxyproline content in mice with chronic CCl_4-induced hepatic fibrosis.

Previous CB_1 antagonists were designed to easily penetrate the blood–brain barrier to antagonize the CB_1 receptors in the central nervous system. Although rimonabant was the first effective CB_1 antagonist used to treat hepatic

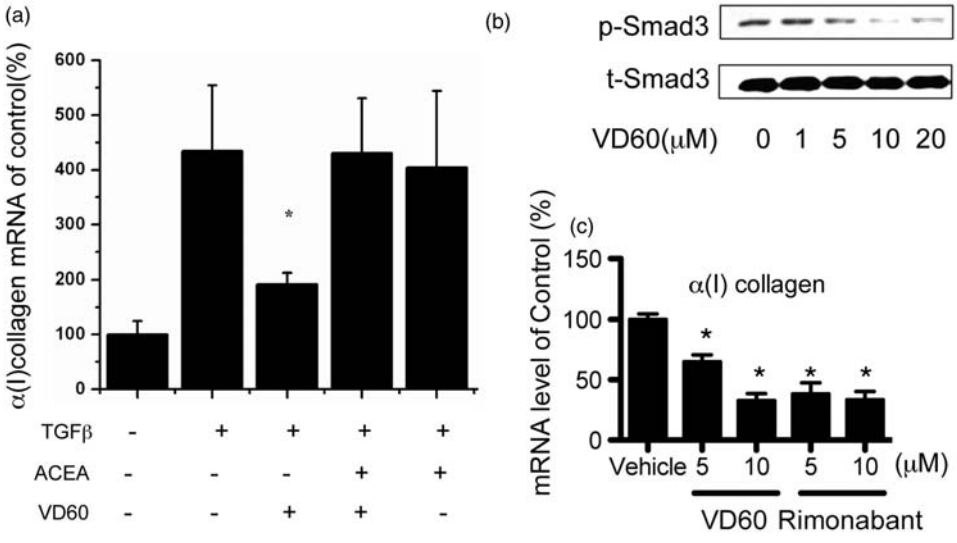

Figure 3 VD60 attenuates key fibrogenesis-involved proteins in LX-2 cells by inhibiting CB_1. (a) LX-2 cells were incubated with 10 μM VD60 in the presence of 2.5 ng/mL $TGF\beta_1$ for 24 h. The ability of VD60 to inhibit procollagen I α_2 mRNA expression was determined by real-time PCR assay. Co-incubation with ACEA (5 μM) abolished the VD60-induced reduction in mRNA levels (* indicates $P < 0.05$ versus control). Data are expressed as the mean ± SEM of three independent experiments. (b) In the LX-2 cells treated with indicated compounds for 48 h, the phosphorylation levels of Smad3 were inhibited by VD60. (c) LX-2 cells were treated with indicated compounds for 24 h in the presence of 2.5 ng/mL $TGF\beta_1$ to examine the procollagen I α_2 mRNA expression with real-time PCR assay (* indicates $P < 0.05$ versus control).

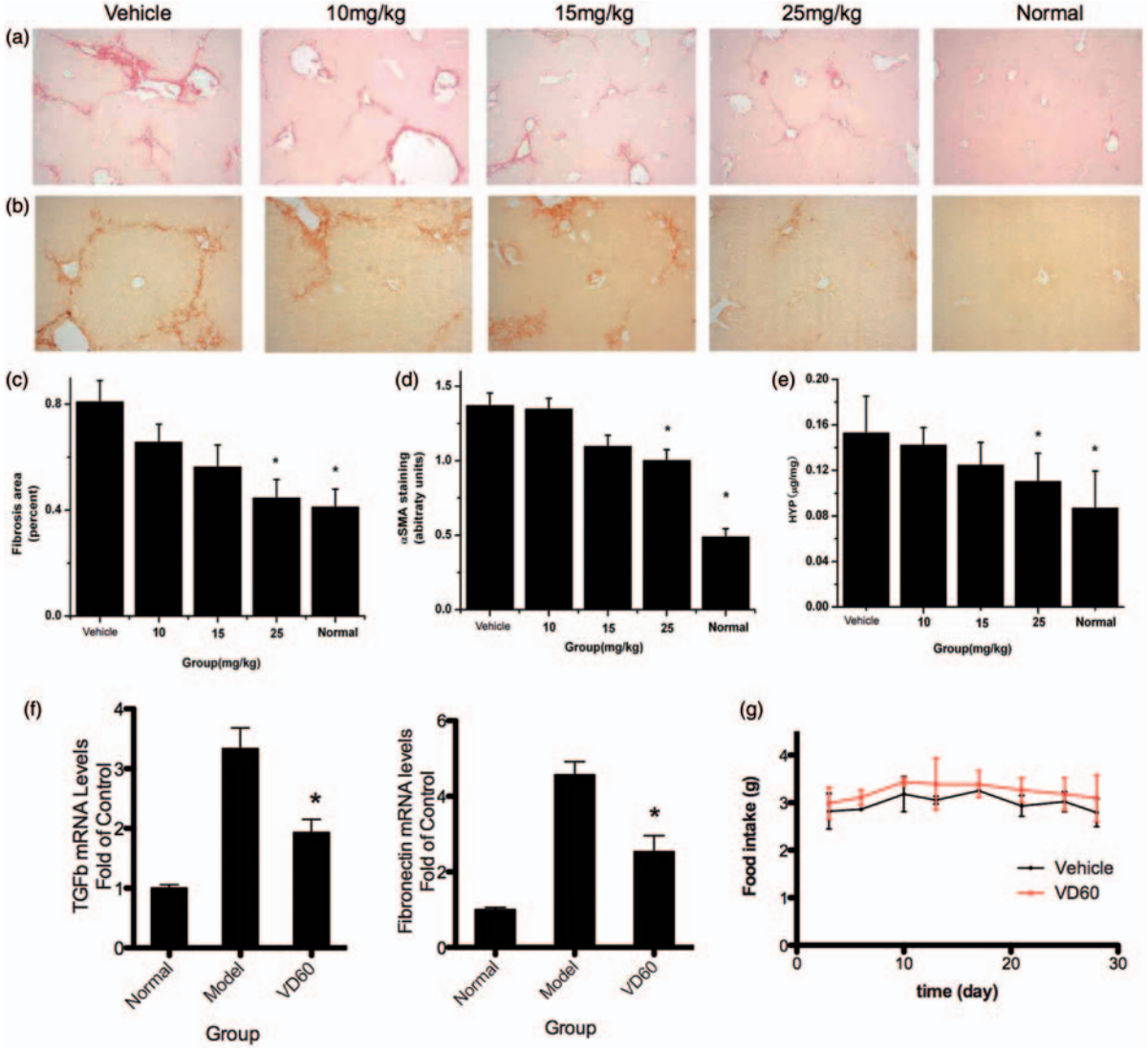

Figure 4 VD60 attenuates liver fibrogenesis in CCl_4-induced fibrotic mice. Mice ($n = 8$ per group) were induced with CCl_4 for 4 weeks to produce hepatofibrosis, and different concentrations of VD60 (0, 10, 15, and 25 mg/kg) were administered i.p. every day. (a) Sirius red staining (collagen fibers) was used to detect the fibrotic area. (b) Immunostaining for α-SMA-positive cells in mouse livers. (c) Quantitative data for Sirius red staining indicated that the fibrotic area in the VD60 (25 mg/kg) treated mice was significantly smaller compared with the vehicle group. *$P < 0.05$ versus vehicle group. (d) α-SMA staining data showed that VD60 treatment dose dependently reduced the expression of α-SMA in CCl_4-induced fibrotic livers. *$P < 0.05$ versus vehicle group. (e) Hydroxyproline (HYP) deposition assay was performed in the livers after 4 weeks of VD60 administration. The hydroxyproline content in the 25 mg/kg treated group was significantly reduced compared to the control liver fibrosis group. *$P < 0.05$ versus vehicle group. (f) Real-time PCR detection was performed and the mRNA levels of TGFb and fibronectin were obviously reduced in 25 mg/kg VD60 treated group. *$P < 0.05$ versus model group. (g) There was no obvious change of the food intake in 25 mg/kg VD60-treated mice during 4-week treatment . (A color version of this figure is available in the online journal.)

fibrosis, the compound induced severe depression and suicidal tendencies. However, growing evidence indicates that CB_1 antagonists not only work in the central nervous system but also target peripheral CB_1. Novel CB_1 antagonists should primarily accumulate in the peripheral tissues to reduce the psychological side effects of these antagonists. VD60 is a peripheral CB_1 antagonist that accumulates at much higher concentrations in the blood plasma than in the brain, suggesting VD60 acts as a peripheral CB_1 antagonist. This characteristic should reduce the central nervous system side effects of VD60 when using the compound to treat peripheral diseases such as hepatic fibrosis.

In conclusion, we have designed a novel peripheral CB_1 antagonist VD60, which demonstrates efficient inhibitory activity against hepatic fibrosis progression, and have investigated the underlying mechanisms of action for this new compound. Our study provides new insights into the antifibrotic application for this novel pharmacophore of a CB_1 antagonist. VD60 could be used as a lead compound for further antifibrotic agent development.

Author contributions: YW and XW designed studies; YW and XW performed research; YW, XW, and XLK analyzed data; YW, XW, and XLK wrote the paper.

ACKNOWLEDGMENT

This work was supported by the National Natural Science Foundation of China (81100680, 81201715).

REFERENCES

1. Bataller R, Brenner DA. Liver fibrosis. *J Clin Invest* 2005;**115**:209–18
2. Gines P, Cardenas A, Arroyo V, Rodes J. Current concepts—Management of cirrhosis and ascites. *N Engl J Med* 2004;**350**:1646–54
3. Lotersztajn S, Julien B, Teixeira-Clerc F, Grenard P, Mallat A. Hepatic fibrosis: Molecular mechanisms and drug targets. *Annu Rev Pharmacol Toxicol* 2005;**45**:605–28
4. Pacher P, Batkai S, Kunos G. The endocannabinoid system as an emerging target of pharmacotherapy. *Pharmacol Rev* 2006;**58**:389–462
5. Farquhar-Smith WP, Egertova M, Bradbury EJ, McMahon SB, Rice AS, Elphick MR. Cannabinoid CB(1) receptor expression in rat spinal cord. *Mol Cell Neurosci* 2000;**15**:510–21
6. Tsou K, Brown S, Sanudo-Pena MC, Mackie K, Walker JM. Immunohistochemical distribution of cannabinoid CB1 receptors in the rat central nervous system. *Neuroscience* 1998;**83**:393–411
7. van der Poorten D, Shahidi M, Tay E, Sesha J, Tran K, McLeod D, Milliken JS, Ho V, Hebbard LW, Douglas MW, George J. Hepatitis C virus induces the cannabinoid receptor 1. *PLoS One* 2010;**5**:ii: e12841
8. Patsenker E, Stoll M, Millonig G, Agaimy A, Wissniowski T, Schneider V, Mueller S, Brenneisen R, Seitz HK, Ocker M, Stickel F. Cannabinoid receptor type i modulates alcohol-induced liver fibrosis. *Mol Med* 2011;**17**:1285–94
9. Trebicka J, Racz I, Siegmund SV, Cara E, Granzow M, Schierwagen R, Klein S, Wojtalla A, Hennenberg M, Huss S, Fischer HP, Heller J, Zimmer A, Sauerbruch T. Role of cannabinoid receptors in alcoholic hepatic injury: Steatosis and fibrogenesis are increased in CB2 receptor-deficient mice and decreased in CB1 receptor knockouts. *Liver Int* 2011;**31**:860–70
10. Siegmund SV, Schwabe RF. Endocannabinoids and liver disease. II. Endocannabinoids in the pathogenesis and treatment of liver fibrosis. *Am J Physiol Gastrointest Liver Physiol* 2008;**294**:G357–62
11. Parfieniuk A, Flisiak R. Role of cannabinoids in chronic liver diseases. *World J Gastroenterol* 2008;**14**:6109–14
12. Izzo AA, Camilleri M. Emerging role of cannabinoids in gastrointestinal and liver diseases: Basic and clinical aspects. *Gut* 2008;**57**:1140–55
13. Lotersztajn S, Teixeira-Clerc F, Julien B, Deveaux V, Ichigotani Y, Manin S, Tran-Van-Nhieu J, Karsak M, Zimmer A, Mallat A. CB2 receptors as new therapeutic targets for liver diseases. *Br J Pharmacol* 2008;**153**:286–9
14. Chen SW, Wu BY, Xu SP, Fan KX, Yan L, Gong Y, Wen JB, Wu DH. Suppression of CB1 cannabinoid receptor by lentivirus mediated small interfering RNA ameliorates hepatic fibrosis in rats. *PLoS One* 2012;**7**(12): e50850
15. Teixeira-Clerc F, Julien B, Grenard P, Van Nhieu JT, Deveaux V, Li LY, Serriere-Lanneau V, Ledent C, Mallat A, Lotersztajn S. CB1 cannabinoid receptor antagonism: A new strategy for the treatment of liver fibrosis. *Nat Med* 2006;**12**:671–6
16. Giannone FA, Baldassarre M, Domenicali M, Zaccherini G, Trevisani F, Bernardi M, Caraceni P. Reversal of liver fibrosis by the antagonism of endocannabinoid CB1 receptor in a rat model of CCl(4)-induced advanced cirrhosis. *Lab Invest* 2011;**92**:384–95
17. Domenicali M, Caraceni P, Giannone F, Pertosa AM, Principe A, Zambruni A, Trevisani F, Croci T, Bernardi M. Cannabinoid type 1 receptor antagonism delays ascites formation in rats with cirrhosis. *Gastroenterology* 2009;**137**:341–49
18. Pi-Sunyer FX, Aronne LJ, Heshmati HM, Devin J, Rosenstock J. Effect of rimonabant, a cannabinoid-1 receptor blocker, on weight and cardiometabolic risk factors in overweight or obese patients: RIO-North America: A randomized controlled trial. *JAMA* 2006;**295**:761–75
19. Van Gaal LF, Rissanen AM, Scheen AJ, Ziegler O, Rossner S. Effects of the cannabinoid-1 receptor blocker rimonabant on weight reduction and cardiovascular risk factors in overweight patients: 1-year experience from the RIO-Europe study. *Lancet* 2005;**365**:1389–97
20. Despres JP, Golay A, Sjostrom L. Effects of rimonabant on metabolic risk factors in overweight patients with dyslipidemia. *N Engl J Med* 2005;**353**:2121–34
21. Lange JH, Kruse CG. Keynote review: Medicinal chemistry strategies to CB1 cannabinoid receptor antagonists. *Drug Discov Today* 2005;**10**:693–702
22. Pettersson H, Bulow A, Ek F, Jensen J, Ottesen LK, Fejzic A, Ma JN, Del Tredici AL, Currier EA, Gardell LR, Tabatabaei A, Craig D, McFarland K, Ott TR, Piu F, Burstein ES, Olsson R. Synthesis and evaluation of dibenzothiazepines: A novel class of selective cannabinoid-1 receptor inverse agonists. *J Med Chem* 2009;**52**:1975–82
23. Planaguma A, Claria J, Miquel R, Lopez-Parra M, Titos E, Masferrer JL, Arroyo V, Rodes J. The selective cyclooxygenase-2 inhibitor SC-236 reduces liver fibrosis by mechanisms involving non-parenchymal cell apoptosis and PPARgamma activation. *FASEB J* 2005;**19**:1120–2
24. Gonsiorek W, Lunn C, Fan X, Narula S, Lundell D, Hipkin RW. Endocannabinoid 2-arachidonyl glycerol is a full agonist through human type 2 cannabinoid receptor: Antagonism by anandamide. *Mol Pharmacol* 2000;**57**:1045–50
25. Price MR, Baillie GL, Thomas A, Stevenson LA, Easson M, Goodwin R, McLean A, McIntosh L, Goodwin G, Walker G, Westwood P, Marrs J, Thomson F, Cowley P, Christopoulos A, Pertwee RG, Ross RA. Allosteric modulation of the cannabinoid CB1 receptor. *Mol Pharmacol* 2005;**68**:1484–95
26. Zhou Y, Wu H, Li S, Chen Q, Cheng XW, Zheng J, Takemori H, Xiong ZQ. Requirement of TORC1 for late-phase long-term potentiation in the hippocampus. *PLoS One* 2006;**1**:e16
27. Julien B, Grenard P, Teixeira-Clerc F, Van Nhieu JT, Li L, Karsak M, Zimmer A, Mallat A, Lotersztajn S. Antifibrogenic role of the cannabinoid receptor CB2 in the liver. *Gastroenterology* 2005;**128**:742–55
28. Skehan P, Storeng R, Scudiero D, Monks A, McMahon J, Vistica D, Warren JT, Bokesch H, Kenney S, Boyd MR. New colorimetric cytotoxicity assay for anticancer-drug screening. *J Natl Cancer Inst* 1990;**82**:1107–12
29. Anan A, Baskin-Bey ES, Bronk SF, Werneburg NW, Shah VH, Gores GJ. Proteasome inhibition induces hepatic stellate cell apoptosis. *Hepatology* 2006;**43**:335–44
30. Bass DA, Parce JW, Dechatelet LR, Szejda P, Seeds MC, Thomas M. Flow cytometric studies of oxidative product formation by neutrophils: A graded response to membrane stimulation. *J Immunol* 1983;**130**:1910–7
31. Jinnin M, Ihn H, Tamaki K. Characterization of SIS3, a novel specific inhibitor of Smad3, and its effect on transforming growth factor-beta1-induced extracellular matrix expression. *Mol Pharmacol* 2006;**69**:597–607
32. Sakaida I, Matsumura Y, Kubota M, Kayano K, Takenaka K, Okita K. The prolyl 4-hydroxylase inhibitor HOE 077 prevents activation of Ito cells, reducing procollagen gene expression in rat liver fibrosis induced by choline-deficient L-amino acid-defined diet. *Hepatology* 1996;**23**:755–63
33. Mayr B, Montminy M. Transcriptional regulation by the phosphorylation-dependent factor CREB. *Nat Rev Mol Cell Biol* 2001;**2**:599–609
34. Galve-Roperh I, Rueda D, Gomez del Pulgar T, Velasco G, Guzman M. Mechanism of extracellular signal-regulated kinase activation by the CB(1) cannabinoid receptor. *Mol Pharmacol* 2002;**62**:1385–92
35. Hillard CJ, Manna S, Greenberg MJ, DiCamelli R, Ross RA, Stevenson LA, Murphy V, Pertwee RG, Campbell WB. Synthesis and characterization of potent and selective agonists of the neuronal cannabinoid receptor (CB1). *J Pharmacol Exp Ther* 1999;**289**:1427–33
36. Di Marzo V, Goparaju SK, Wang L, Liu J, Batkai S, Jarai Z, Fezza F, Miura GI, Palmiter RD, Sugiura T, Kunos G. Leptin-regulated endocannabinoids are involved in maintaining food intake. *Nature* 2001;**410**:822–5
37. Herling AW, Kilp S, Elvert R, Haschke G, Kramer W. Increased energy expenditure contributes more to the body weight-reducing effect of rimonabant than reduced food intake in candy-fed Wistar rats. *Endocrinology* 2008;**149**:2557–66
38. Gary-Bobo M, Elachouri G, Gallas JF, Janiak P, Marini P, Ravinet-Triflou C, Chabbert M, Cruccioli N, Pfersdorff C, Roque C, Arnone M, Croci T, Soubrie P, Oury-Donat F, Maffrand JP, Scatton B, Lacheretz F, Le Fur G, Herbert JM, Bensaid M. Rimonabant reduces obesity-associated hepatic steatosis and features of metabolic syndrome in obese Zucker fa/fa rats. *Hepatology* 2007;**46**:122–9

39. Jeong WI, Osei-Hyiaman D, Park O, Liu J, Batkai S, Mukhopadhyay P, Horiguchi N, Harvey-White J, Marsicano G, Lutz B, Gao B, Kunos G. Paracrine activation of hepatic CB1 receptors by stellate cell-derived endocannabinoids mediates alcoholic fatty liver. *Cell Metabolism* 2008;**7**:227–35
40. Deleve LD, Wang X, Kanel GC, Atkinson RD, McCuskey RS. Prevention of hepatic fibrosis in a murine model of metabolic syndrome with nonalcoholic steatohepatitis. *Am J Pathol* 2008;**173**:993–1001
41. Osei-Hyiaman D, Liu J, Zhou L, Godlewski G, Harvey-White J, Jeong WI, Batkai S, Marsicano G, Lutz B, Buettner C, Kunos G. Hepatic CB(1) receptor is required for development of diet-induced steatosis, dyslipidemia, and insulin and leptin resistance in mice. *J Clin Invest* 2008;**118**:3160–9

(Received July 6, 2013, Accepted October 16, 2013)